

MILITARY TECHNICAL COLLEGE
CAIRO - EGYPT1st INTERNATIONAL CONF.
ON
ELECTRICAL ENGINEERING

Plane Wave Scattering From Microstrip Array of Patches at Arbitrary Incidence

A.M.M.A. Allam^{*1}

Abstract

This paper presents a discrete domain analysis for plane wave scattering from passive microstrip array of patches at arbitrary incidence over a wide frequency band. The analysis shows the effect of the patch size on the resonance of the scattered higher modes of the structure. The dips in the reflection coefficient characteristic curves at different angles of incidence correlate the level of these modes. The effect of the grating lobes onset on the reflection characteristics is also depicted.

KEY WORDS

Antennas, microstrip antennas, scattering and radiation.

1. INTRODUCTION

The basic characteristics and design procedures for microstrip arrays of patches as a transmitting antennas can be found in many articles [1,2]. This chance is not available for the designer of microstrip arrays for receivers. The main interest of a few articles that may help in this trend is studying the RCS [3,4] and RCS reduction of some structures [5-7]. In transmitting mode, the efficiency is higher as much as the level of the bounded waves are lower. The basic rule in design of transmitting antenna is avoiding resonance of these waves in the frequency band of interest over the scanning sector. In receiving mode, the signal power has to be coupled from the space to the feeder by the microstrip structure. For high efficiency receiving antennas, the reflection from the air-substrate interface as well as the level of the bounded waves have to be minimum.

This paper is a continuation for the work done on the plane wave scattering from microstrip passive arrays as bounded wave modes and grating lobes [8]. Rectangular patch arrays on

¹ Ass.Prof., Egyptian Armed Force.

square lattice with different patch dimensions are considered. The scattering characteristics are investigated for different angles of incidence, normal, 30° & 45° TE & TM. The problem of active arrays is not presented.

2. FORMULATION

The integral equations for an infinite array of rectangular microstrip elements at the air-substrate interface (x-y plane) for the structure shown in Fig. 1 are

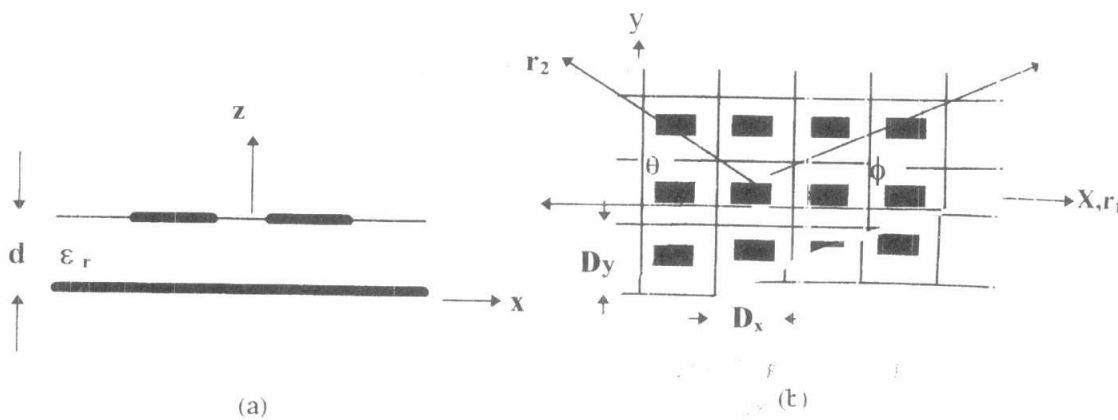


Fig. 1 The geometry of microstrip array of patches
a) side view b) top view

$$\begin{aligned}
 E_x &= E_x^i + E_x^r + \frac{1}{4\pi^2} \iint (\tilde{G}_{xx} \tilde{J}_x + \tilde{G}_{xy} \tilde{J}_y) e^{ik_x x} e^{ik_y y} dk_x dk_y \\
 E_y &= E_y^i + E_y^r + \frac{1}{4\pi^2} \iint (\tilde{G}_{yx} \tilde{J}_x + \tilde{G}_{yy} \tilde{J}_y) e^{ik_x x} e^{ik_y y} dk_x dk_y
 \end{aligned}
 \tag{1}$$

where E_x and E_y are the total electric field components, E_x^i and E_y^i are the incident electric field components E_x^r and E_y^r are the reflected field components due to the incident plane wave without the presence of the array elements, J_x and J_y are the surface currents induced on the array elements, and \tilde{G}_{xx} , \tilde{G}_{xy} , \tilde{G}_{yx} and \tilde{G}_{yy} , are the Green's functions of the pertinent structure. The tilde over the quantities denotes the quantities in the (k_x, k_y) spectral domain.

The Green's functions in case of lossless dielectric substrate are given, in a form similar to that in [9], as:

$$\begin{aligned}
 \tilde{G}_{xx}(k_x, k_y) &= \frac{Z_o}{k_o \beta^2} \left(\frac{i k_1 k_2 k_x^2}{\epsilon_r k_2 \Gamma_1 - i k_1} + \frac{k_o^2 k_y^2}{i k_1 \Gamma_2 - k_2} \right) \\
 \tilde{G}_{yy}(k_x, k_y) &= \frac{Z_o}{k_o \beta^2} \left(\frac{i k_1 k_2 k_y^2}{\epsilon_r k_2 \Gamma_1 - i k_1} + \frac{k_o^2 k_x^2}{i k_1 \Gamma_2 - k_2} \right) \\
 \tilde{G}_{xy}(k_x, k_y) &= \frac{Z_o}{k_o \beta^2} \left(\frac{i k_1 k_2 k_x k_y}{\epsilon_r k_2 \Gamma_1 - i k_1} - \frac{k_o^2 k_x k_y}{i k_1 \Gamma_2 - k_2} \right) \\
 \tilde{G}_{yx}(k_x, k_y) &= \tilde{G}_{xy}(k_x, k_y)
 \end{aligned} \tag{2}$$

where

$$\Gamma_1(k_x, k_y) = -\cos(k_1 d) / \sin(k_1 d) = -\Gamma_2(k_x, k_y),$$

$$k_1^2 = \epsilon_r k_o^2 - \beta^2, \quad k_2^2 = k_o^2 - \beta^2, \quad \beta^2 = k_x^2 + k_y^2$$

(Imag. of k_1 and $k_2 < 0$), k_o is the free space wave number, ϵ_r is the relative permittivity of the substrate, d is the substrate thickness, and Z_o is the free space intrinsic impedance.

One of the efficient techniques for solving Eqn.(1) is the iterative scheme of the CG-FFT [10]. In this discrete technique, the domain of periodicity is segmented in directions that minimize the total number of segments, and outlines the array elements accurately. The general form of the Discrete Fourier Transform (DFT) equation is given by [11]:

$$\begin{aligned}
 F_{m_1, m_2} &= \frac{1}{N_1 N_2} \sum_{n_1} \sum_{n_2} f_{n_1, n_2} e^{-i2\pi \left(\frac{m_1 n_1}{N_1} - \frac{m_2 n_2}{N_2} - m_2 n_2 \frac{\Delta x_2}{Dx_1} (\cotan(\theta) + \cotan(\phi)) \right)}; \\
 n_1 &= 0, N_1 - 1, \quad n_2 = 0, N_2 - 1
 \end{aligned} \tag{3}$$

where ϕ is the angle between the directions of periodicity, and θ defines the directions of segmentation \hat{r}_1 and \hat{r}_2 ; see Fig.1.b. In Eqn.(3), N_1 and N_2 are the number of segments in \hat{r}_1 and \hat{r}_2 , respectively, and the locations of the DFT coefficients are:

$$\begin{aligned}
 k_x &= m_1 \frac{2\pi}{Dx} + k_x^i, \quad k_y = m_2 \frac{2\pi}{Dy} - m_1 \frac{2\pi}{Dx} \cotan(\phi) + k_y^i, \\
 \text{for } -\frac{N_1}{2} &\leq m_1 < \frac{N_1}{2}, \quad \text{and } -\frac{N_2}{2} \leq m_2 < \frac{N_2}{2}
 \end{aligned} \tag{4}$$

where k_x^i and k_y^i are the incident wave numbers in x and y directions. The inverse DFT can be written as:

$$f_{n_1, n_2} = \sum_{m_1} \sum_{m_2} F_{m_1, m_2} e^{i2\pi \left(\frac{m_1 n_1}{N_1} - \frac{m_2 n_2}{N_2} - m_2 n_2 \frac{\Delta x_2}{Dx_1} (\cotan(\theta) + \cotan(\phi)) \right)} \tag{5}$$

From Eqns.(3) and (4), the number of Floquet's modes are N_1 and N_2 in \hat{k}_x and \hat{k}_y respectively. Hence, Eqn.(1) can be rewritten as:

$$E_x = E_x^i + E_x^r + \sum_{m_1, m_2} E_{x(m_1, m_2)}^s$$

$$E_y = E_y^i + E_y^r + \sum_{m_1, m_2} E_{y(m_1, m_2)}^s$$

where E^s denotes the scattered field component. The reflection coefficient (R)

$$R = \frac{E_{x,y(0,0)}^s + E_{x,y}^r}{E_{x,y}^i}$$

for x-/y-polarized incident plane wave.

One important notice is that this discrete technique is similar to the method of moment using Galerkin procedure with subdomain basis function of pulses. The number of current basis function is the number of segments that outline the conductor, while the number of Floquet's modes equals the number of segments of a unit cell. As illustrated in [12], it provides an accurate solution with a stable convergence in terms of the used number of Floquet's modes.

3.RESULTS

Consider a structure of periodic microstrip array as shown in Fig.1 of rectangular patches with sides of length a_x and a_y parallel to x and y axes, $\phi=90^\circ$, $D_x=D_y=.5\text{Cm}$. The substrates is assumed lossless dielectric with $\epsilon_r=2.55$ & 12.55 and $d=.06\text{Cm}$. The numerical results are obtained by sampling the unit cell of the array into 16 samples in both x & y directions ($\theta=90^\circ$): i.e. 16 Floquet's modes are considered in each direction.

Assume that the structure is illuminated by a normal incident x- polarized plane wave. The scattering of the higher modes(1,0), (1,1), and (2,0) in case of different patch sizes with $\epsilon_r=2.55$ is shown in Figs.2.a,b and c ($a_x \times a_y$), $0.031\text{Cm} \times 0.031\text{Cm}$, $0.062\text{Cm} \times 0.062\text{Cm}$, $0.44\text{Cm} \times 0.25\text{Cm}$ and $0.44\text{Cm} \times 0.38\text{Cm}$. The arrows depicted in figures represent the pole frequencies of the Green's function (Eqn.2), the resonance of the higher in case of unloaded grounded dielectric slab. In the presence of the patches, it is found that the resonance frequencies of these modes depend on the patch size. As the patch dimensions are getting smaller, the modes resonance frequencies are approaching the pole frequencies of those modes otherwise the modes resonance frequencies appear earlier. These results limit the approximations that are commonly applied in the analysis of an infinite phased arrays where the effect of the patches is ignored in computing the exciting surface fields [13,14].

The effect both of the higher modes and the grating lobes on the scattering characteristics of microstrip array of patches is demonstrated in Figs.3.a and b in case of patch dimensions $0.44\text{Cm} \times 0.25\text{Cm}$ with $\epsilon_r=2.55$ illuminated by oblique incident plane wave at 45° TE & TM and 30° TE & TM respectively. The reflection coefficients R of the dominant mode for normal incidence are

depicted on each graph by solid lines. The figures show that the structure reflects all the normal incident wave in the frequency band less than the first grating lobe onset frequency, $f_{GL}=60$ GHz. Beyond f_{GL} , the grating lobes onset in both E- and H-planes reduces the level of the reflected dominant mode. Also the amplitudes of the scattering higher modes for the chosen structure have a negligible effect on the reflection characteristics at normal incidence. In the case of oblique incidence 30° and 45° , more narrow dips were found. At these angles of incidence the resonance of the higher modes and the first grating lobe onset start at lower frequencies than that the case of normal incidence (the higher modes start in both E&H planes at 28.7 GHz and 26.1 for 30° and 45° incidences respectively, on the other hand the grating lobes start at 40 GHz and 35.2 GHz for 30° and 45° incidences. It is clear that the dips in R curves correlate the level of the modes (0,+1), (+1,0) and (+1,-1) as shown in Fig.4. In this figure the case for the absolute values of E_x in these modes for $a_x=.44$ Cm and $a_y=.25$ Cm at 30° TE incidence are illustrated. It is very important to point out that the resonance of the modes (0,-1) has a negligible effect on the corresponding R curves, which means that the power of these modes (TE- modes) of the pertinent structure is very small in this band.

As ϵ_r is increased, more higher order modes are supported. Fig.5 show reflection curves of the same structure and geometry but for $\epsilon_r=12.55$ for 30° TE & TM incidences. It shows multi-dips in the reflection curves for the different cases. These dips were found to correlate also the levels of the modes (-1,0), (+1,0), (+1,-1) and (-2,0) as above over the whole frequency band of interest as shown in Fig.6, for the case 30° TM. One notices that at higher frequencies no wide drop in R curves for the considered case has been found. This is due to the cancellation of the multi-higher modes inside the structure and the low levels of the grating lobes .

4.CONCLUSION

The reflected power from the space-dielectric interface of a microstrip array of patches is minimum when the higher modes resonance occurs and the resonance frequencies of these modes are dependent on the patch size. This result contradicts the basic requirement for the microstrip array in receiving mode, where the presence of resonance minimize the power that can be delivered through the feeder. Therefore, the feeder of receiving antennas must have a major rule on the scattering characteristics of the microstrip structure.

The analysis shows the correlation between the resonance of the higher modes and the dips in the reflection curves for different angle of incidences.

REFERENCES:

- [1] Liu C., Hessel A., and Shmoys J., "Performance of prob-feed microstrip-patch element phased arrays", IEEE Trans. Antennas Propagat., Vol. AP-36, No.11, Nov. 1988, PP.1501-1509.
- [2] Nehra C., Hessel A., Shmoys J., and Stalzer H., "Prob-fed strip-element microstrip phased arrays: E- and H-plane scan resonance and broadbanding guidelines", IEEE Trans. Antennas Propagat., Vol. AP-43, No.11, Nov. 1995, PP.1270-1280.
- [3] Liu C., Hessel A., Hanfling J., and Usoff J., "Plane wave reflection from microstrip-patch arrays-

- theory and experiment", IEEE Trans. Antennas Propagat., Vol. AP- , No. , 1985, PP.426-435.
- [4] Newman E., and Forrai D., " Scattering from microstrip patch", IEEE Trans. Antennas Propagat., Vol. AP-35, No.3, March 1987, PP.245-250.
- [5] Pozar D., "Microstrip antennas and arrays on chiral substrates", IEEE Trans. Antennas Propagat., Vol.AP-40, No.10, Oct. 1992, PP.1260-1263.
- [6] Pozar D., " Radiation and scattering characteristics of microstrip antennas on normally biased ferrite substrates", IEEE Trans. Antennas Propagat., Vol.AP-40, No.9, Sept. 1992, PP.1084-1092.
- [7] Yang H., Castanecla J., and Alexopoulos G., "The RCS of a microstrip patch on arbitrary biased ferrite substrate", IEEE Trans. Antennas Propagat., Vol.AP-41, No.12, Dec. 1993, PP. 1610-1614.
- [8] Ragab A.S., Mokhtar M., Allam A.M. and Ibrahim S.M., "Plane wave scattering from microstrip passive arrays", Proc. Of 14th Nat. Radio Science Conf., Cairo, Egypt, 1997, PP1-8 (B3)
- [9] Jin J., and Volakis J., " Electromagnetic scattering by a perfectly conducting patch array on a dielectric slab", IEEE Trans. Antennas Propagat., Vol.AP-38, No.4, April 1990, PP.556-563.
- [10] Peters, T.J. and Volakis, J.J.: "Application of a Conjugate Gradient FFT method to scattering from thin planar material plates", IEEE Trans. Antennas Propagat., Vol.AP-36, No.4, 1988, PP.518-526.
- [11] Mokhtar, M.: "Conjugate Gradient analysis of hexagonally sampled FSS", Advances in Modelling & Analysis, B, AMSE Press, Vol.33, No.1, 1995, PP.9-19.
- [12] Allam A.M. and Mokhtar M., "Convergence in the analysis of frequency selective surfaces of linear dipoles", Proc. Of 13th Nat. Radio Science Conf., Cairo, Egypt, 1996, PP1-8 (B3)
- [13] Tsalamenges, J. L., "TE- scattering by conducting strips right on the planar interface of a three - layered Medium", IEEE Trans. Antennas Propagat., Vol. AP. 41 No. 12, December 1993, pp.1650-1685.
- [14] Pozar, D. M. "Analysis of an infinite array of aperture coupled microstrip patches", "IEEE Trans. Antennas Propagat., Vol. AP. 37 No. 4, December 1989, pp.418-425.

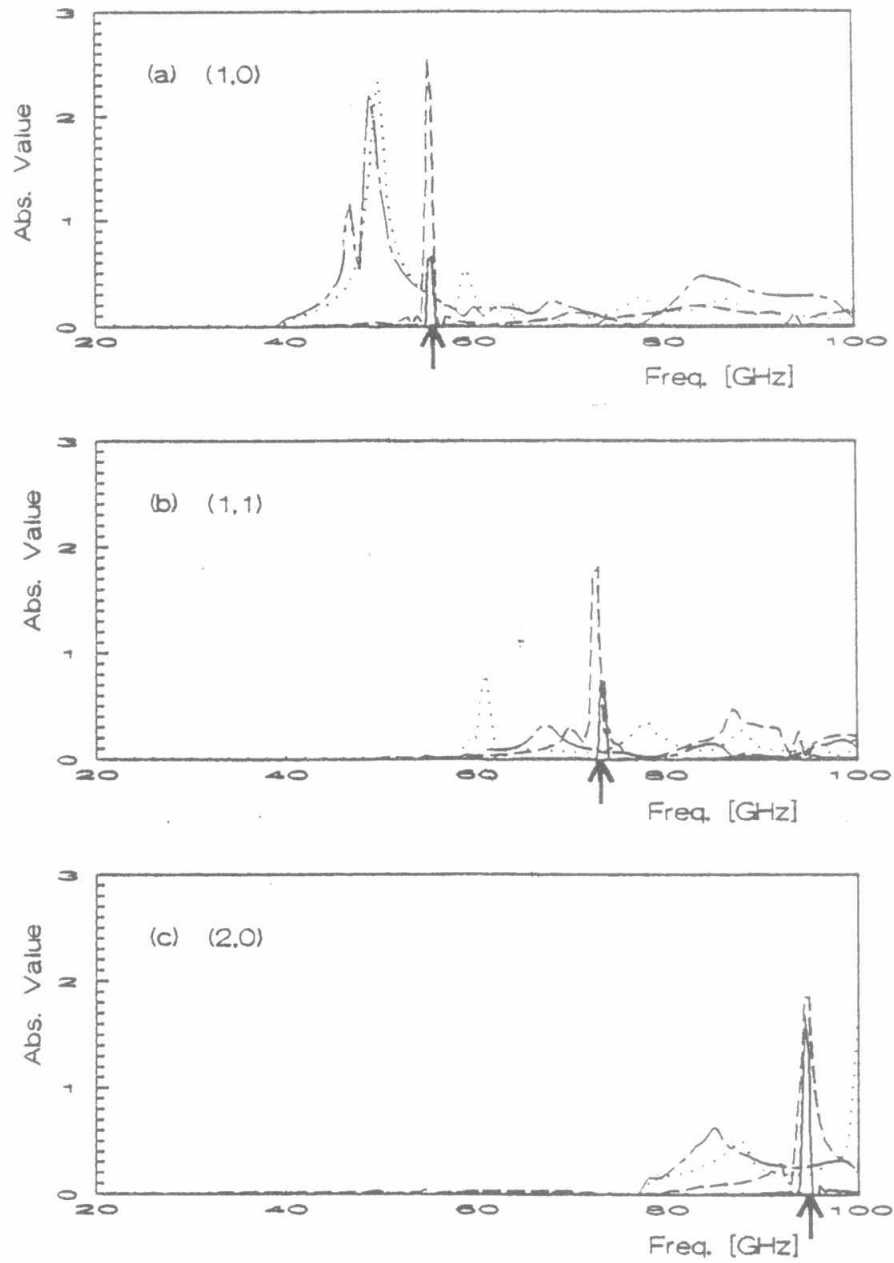


Fig.2 The amplitudes of the higher modes at normal incidence inside the structure for different patch sizes with $d = 2.55$

$a_x = 0.031\text{Cm}$, $a_y = 0.031\text{Cm}$ $a_x = 0.440\text{Cm}$, $a_y = 0.250\text{Cm}$
 $a_x = 0.062\text{Cm}$, $a_y = 0.062\text{Cm}$ $a_x = 0.440\text{Cm}$, $a_y = 0.380\text{Cm}$

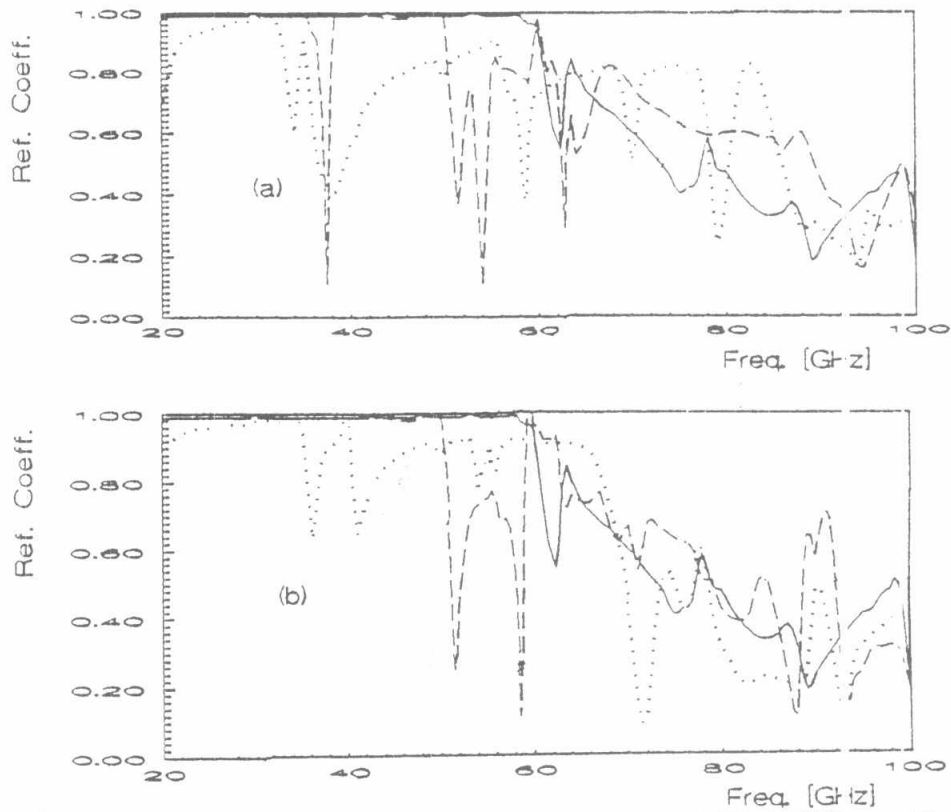


Fig.3 The ref. coef. vs. freq. for patch size .44CmX.25Cm with $\epsilon_r = 2.55$. — normal incidence, --- TE, TM.
 (a) 45 Degree. (b) 30 Degree.

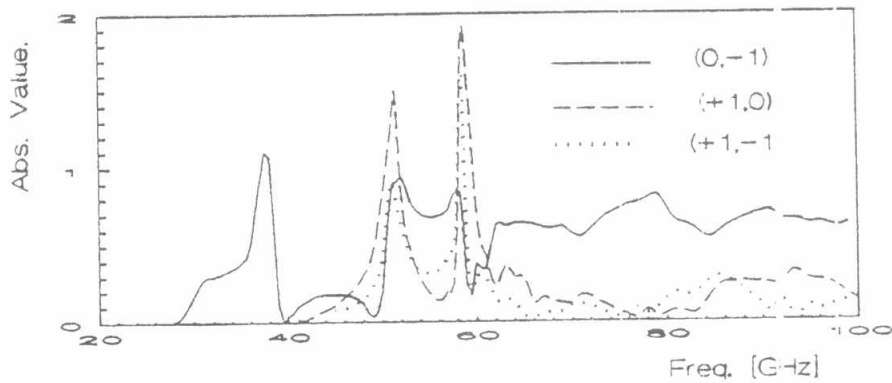


Fig.4 The absolute values of the higher modes for the case of 30°TE in Fig.3b (the dashed line).

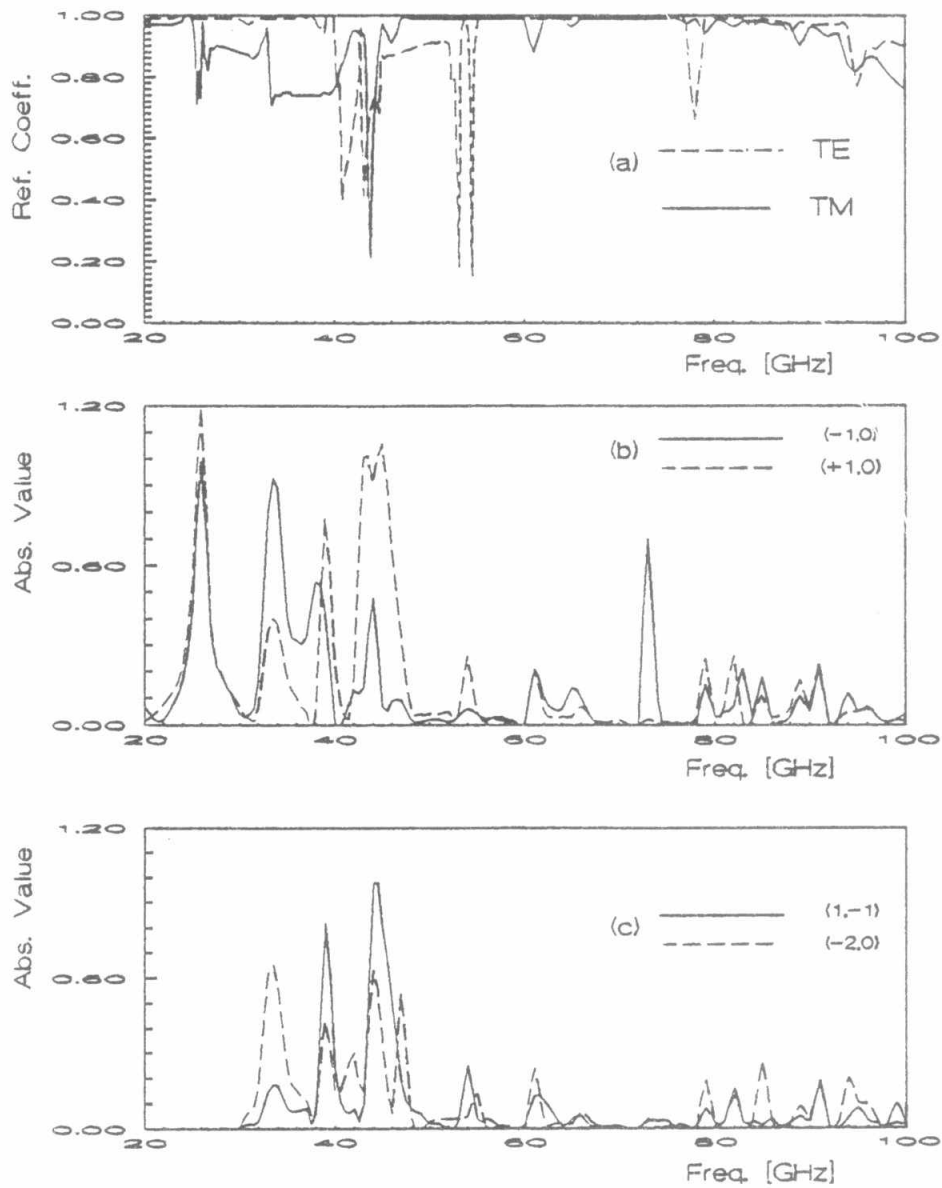


Fig.5 (a) Ref. coeff. vs. freq. for patch size .44CmX.25Cm with $\epsilon_r=12.55$ and $d=.6\text{mm}$ for 30° TE and TM incidences (b) & (c) The absolute values of the higher modes for the 30° TM in (a) (the solid line).

